

Manuscript Number:

Title: Examination of nanocrystalline TiC/amorphous C deposited thin films

Article Type: SI: FAC IV

Keywords: TiC/a:C; magnetron sputtering; structure; mechanical properties; XPS

Corresponding Author: Ms. Nikolett Olah,

Corresponding Author's Institution: MTA TTK MFA

First Author: Nikolett Olah

Order of Authors: Nikolett Olah; Miklos Veres; Attila Sulyok; Miklos Menyhard; Jenő Gubicza; Katalin Balazsi

Abstract: The relationship between structural, chemical and mechanical properties of nanocrystalline TiC / amorphous C thin films was studied. Thin films were deposited by DC magnetron sputtering on oxidized silicon substrates in argon at 25 C° and 0.25 Pa. The input power of the carbon target was 150 W, the input power of the titanium target was varied between 15 and 50 W.

It was found that all thin films consist of a few nanosized columnar TiC crystallites embedded in carbon matrix. The average size of TiC crystallites and the thickness of the carbon matrix have been found to correlate with Ti content. The mechanical properties of the films have been strictly dependent on their structure. The highest values of the nanohardness (~ 66 GPa) and Young's modulus (~ 401 GPa) were observed for the film with the highest TiC content which was prepared at 50 W of Ti target.

Suggested Reviewers: Filiz Cinar Sahin
cinar@itu.edu.tr

Ashok Vasheastha
avaseash@norwich.edu

Csaba Balazsi
csaba.balazsi@bayzoltan.hu

Nikolett Olah

Thin Film Physics department

Institute for Technical Physics and Materials Sciences,

Research Centre for Natural Sciences

Konkoly-Thege ut 29-33, H-1121 Budapest, Hungary

13 November 2013

Dear Editor,

Please find our contribution to Examination of nanocrystalline TiC/amorphous C deposited thin films.

The relationship between structural, chemical and mechanical properties of nanocrystalline TiC / amorphous C (TiC/a:C) thin films was studied. Thin films were deposited by DC magnetron sputtering on oxidized silicon (Si/SiO₂) substrates in argon at 25 C° and 0.25 Pa. The input power of the carbon target was kept at constant value of 150 W while the input power of the titanium target was varied between 15 and 50 W.

It was found that all thin films consist of a few nanosized columnar TiC crystallites embedded in carbon matrix. The average size of TiC crystallites and the thickness of the carbon matrix have been found to correlate with Ti content in the films. The mechanical properties of the films have been strictly dependent on their structure. The highest values of the nanohardness (~ 66 GPa) and Young's modulus (~ 401 GPa) were observed for the film with the highest TiC content which was prepared at the largest input power of Ti target.

The recommended keywords are:

TiC/a:C, magnetron sputtering, structure, mechanical properties, XPS

Looking forward your positive answer.

Sincerely yours,

Nikolett Olah

Summary

The nanocomposite structures will be applied as protective materials or hard coating for multifunctional, industrial and engineering applications [6-8]. In previous studies only a few preparation methods for TiC films have been investigated in details. One of them, the vacuum deposition provides great flexibility for manipulating material chemistry and structure, resulting in films and coatings with special properties

TiC/a:C thin films were deposited by DC magnetron sputtering at 25 °C in argon atmosphere. The films had a thickness of 400 nm and consisted of nanocrystalline TiC and amorphous carbon phases. The average size of TiC crystallites and the thickness of the amorphous carbon matrix strongly depended on deposition parameters, namely on Ti target power. Films deposited at 15 W Ti power consisted of few nanometers small TiC nanocrystallites embedded in a few ten nanometers thick carbon matrix. The increase of Ti content (with increasing Ti power) resulted in larger TiC nanocrystallites and a thinner carbon spacing between the TiC phases. This structural observation correlated with the concentration determined by XPS and EDS measurements. The XPS signal of carbon was decomposed for graphite and carbide according to their binding energies. This observation correlated with Raman measurements. These results confirmed that all Ti atoms were bonded to C.

The nanohardness of TiC/a:C thin films increased proportionately with the TiC crystallite content measured in the films. The highest nanohardness of 66 GPa and elastic modulus of 401 GPa were observed in the film prepared at 50 W, which consisted of 15 nm thick TiC columns separated by a 2-3 nm thin amorphous carbon matrix. The extremely high hardness of the films may be due to the large amount and the small grain size of TiC nanocrystallites.

Examination of nanocrystalline TiC/amorphous C deposited thin films

Nikolett Oláh¹, Miklós Veres², Attila Sulyok¹, Miklós Menyhárd¹, Jenő Gubicza³, Katalin Balázsi¹

¹ *Thin Film Physics Department, Institute for Technical Physics and Materials Science, Research Centre for Natural Sciences, Hungarian Academy of Sciences, Konkoly-Thege M. str. 29-33, 1121 Budapest, Hungary*

² *Institute for Solid State Physics and Optics, Wigner Research Centre for Physics, HAS, Konkoly-Thege M. str. 29-33, 1121 Budapest, Hungary*

³ *Department of Materials Physics, Eötvös Loránd University, P.O.B. 32, 1518 Budapest, Hungary*

Abstract

The relationship between structural, chemical and mechanical properties of nanocrystalline TiC / amorphous C (TiC/a:C) thin films was studied. Thin films were deposited by DC magnetron sputtering on oxidized silicon (Si/SiO₂) substrates in argon at 25 C° and 0.25 Pa. The input power of the carbon target was kept at constant value of 150 W while the input power of the titanium target was varied between 15 and 50 W.

It was found that all thin films consist of a few nanosized columnar TiC crystallites embedded in carbon matrix. The average size of TiC crystallites and the thickness of the carbon matrix have been found to correlate with Ti content in the films. The mechanical properties of the films have been strictly dependent on their structure. The highest values of the nanohardness (~ 66 GPa) and Young's modulus (~ 401 GPa) were observed for the film with the highest TiC content which was prepared at the largest input power of Ti target.

Keywords: TiC/a:C, magnetron sputtering, structure, mechanical properties, XPS

1. Introduction

Nanocomposite coatings composed of crystalline and amorphous nanophases have generated increasing interest. They are implemented in fundamental research and industrial and medical applications as well [1]. These films may be characterized by an unusual combination of mechanical and tribological properties such as high hardness and toughness, superior wear and corrosion resistance, low friction, good thermal conductivity and high electric conductivity [1-5]. Moreover, nanocomposite structures will be applied as protective materials or hard coating for multifunctional, industrial and engineering applications [6-8]. In previous studies only a few preparation methods for TiC films have been investigated in details. One of them, the vacuum deposition provides great flexibility for manipulating material chemistry and structure, resulting in films and coatings with special properties [9]. Y. Wang et al. prepared the films by filtered cathodic vacuum arc deposition [10], El Mel et al. produces them by a hybrid plasma process combining Physical Vapor Deposition (PVD) [11] and H.L. Wang et al. deposited the films by Plasma Enhanced Chemical Vapor Deposition (PECVD) [12]. DC reactive magnetron sputtering and pulsed laser deposition also have been applied to the synthesis of TiC films [13-14]. Sedlackova et al. usually deposited TiC based nanocomposites by magnetron sputtering from Ti and C targets in air ambient [15]. Several nanostructured TiC coating designs exist such as nanoscale multilayer coatings,

1 nanostructured functionally graded coatings [16], because the combination of Ti and C is a
2 relatively easy and cheap process [17].

3 In this study, the structural, chemical and mechanical properties of TiC/a:C thin films
4 deposited by DC magnetron sputtering were investigated. The dependence of thin film
5 properties on the TiC and Ti content were revealed.

6 7 **2. Experimental**

8
9
10 The deposition of TiC based nanocomposites was carried out using a DC magnetron
11 sputtering system in argon atmosphere at the pressure of 0.25 Pa, which consisted of one Ti
12 target and one C target facing each other. The TiC based nanocomposite films were deposited
13 onto 300 nm thick oxidized Si (001) wafers at room temperature. The input power of the C
14 target was kept at a constant value of 150 W while the input power of the Ti target varied
15 between 15 and 50 W. The film thickness was controlled by the deposition time in such a way
16 that all deposited layers had the same thickness of 450 nm.

17
18 Auger Electron Spectroscopy (AES), X-ray Photoelectron Spectroscopy (XPS) and
19 Raman Spectroscopy (RS) were used for matrix characterization. The chemical bonding of the
20 carbon films was investigated by Near-infrared Raman Spectroscopy (NIRS). The
21 measurements have been carried out with a Renishaw1000 B micro-Raman spectrometer
22 using a 785 nm diode laser which served as an excitation source. The structure of the thin
23 films was investigated by transmission electron microscopy (TEM) using a Philips CM-20
24 operated at 200 kV accelerating voltage. The elemental composition of the films was
25 measured by Energy Dispersive Spectroscopy (EDS) using this microscope equipped with a
26 NORAN cooled Ge detector.

27
28
29 The average chemical composition of the films was examined by X-ray Photoelectron
30 Spectroscopy (XPS) using an Al anode. The 5 x 5 mm sized specimens were mounted onto a
31 larger Si wafer and were introduced to the chamber for analysis. The spectra were obtained
32 using special CMA (Cylindrical Mirror Analyzer) with retarding field (type ESA 105 made by
33 Staib Instruments Ltd). Constant energy resolution (1.5 eV) was applied to all measurements.
34 Full depth profile of the whole layers was measured by Auger Electron Spectroscopy (AES)
35 determining the composition along the whole layer thickness and the sputtering speed. Depth
36 profile was measured using 1keV Ar ion beam at a 78° angle of incidence. In case of XPS
37 profile, the ion beam was scanned to such an extent that it evenly sputtered the whole surface
38 of the specimen evenly.

39
40
41 The mechanical characteristics of the TiC thin films were investigated by
42 nanoindentation technique. The nanohardness and elastic modulus of the nanocomposite
43 coatings were evaluated using an UMIS nanoindentation device with a Berkovich diamond
44 indenter. The indentation tests were carried out under the applied load of 1 mN in order to
45 keep the maximum penetration depth below one tenth of the layer thickness (400 nm). Indeed,
46 the maximum indentation depth was between 30-50 nm for all samples. A series of 49
47 penetrations were recorded with the indents arranged in a 7 x 7 matrix with a neighbor
48 spacing of 10 μm.

49 50 51 **3. Results and Discussion**

52 53 *3.1. Chemical properties*

54
55
56
57 The Raman spectra of the TiC/a:C thin films are shown in Fig. 1. The spectra were
58 measured within the wavenumber range of 200 - 2000 cm⁻¹ with 785 nm excitation light. The
59 bands of amorphous carbon were observed for the thin film prepared at minimum Ti power
60
61
62
63
64
65

1 (15 W) between 1000 and 1700 cm^{-1} . The 1420 and 1530 cm^{-1} bands observable in the
2 spectrum correspond to the D (disordered) and G (graphitic) peaks of the amorphous carbon.
3 Both peaks were narrowed with increasing Ti content. It can be explained by the increasing
4 order in the structure and graphitization. Additionally, titanium carbide bands have appeared
5 in the spectra. Five peaks of TiC were observed at 360, 565, 670, 970 and 1075 cm^{-1} . The
6 first three values show a fairly good agreement with the Raman spectrum of $\text{TiC}_{0.67}$ [18]. The
7 differences may arise from the fact that the phase composition might not be the same.
8

9
10 The bulk composition of TiC layers was determined by XPS after removing the
11 surface contamination by ion sputtering. The concentration was calculated by standard
12 evaluation of XPS peaks using a sensitivity factor [19]. Peak shapes were fitted by a sum of
13 Gaussian and Lorentzian after Shirley background subtraction. The XPS signal of carbon
14 was decomposed into graphite and carbide according to their binding energy: graphite 284.0
15 eV and carbide (TiC) 281.8 eV. The difference of binding energy (2.2 eV) was enough to
16 carry out a reasonably reliable decomposition of the detected combined peak. The result of
17 decomposition is shown in Fig. 2. The figure shows that the intensities of graphite line and
18 carbide peaks change oppositely. The thin film consisted of lower graphite and higher carbide
19 content or vice versa.
20

21
22 The composition of films prepared at various Ti target power is summarized in Tab. 1.
23 The lowest Ti content (16 at.%) is produced by the lowest Ti power (15 W). Then, the Ti
24 content increases with the power to the last specimen reaching 40 at.%. The carbon in carbide
25 state increases parallel with the Ti content. The remaining part of carbon is in graphite state
26 that changes oppositely with Ti deposition rate: from ~70 at.% to ~ 8 at.%. It is reasonable to
27 assume that all the Ti atoms reaching the target surface are bound to TiC during the
28 deposition process. The excess carbon remains in graphite state. XPS spectra showed a small
29 but definite Ar signal about 3-4%. It can be excluded that this Ar would be a result of ion
30 sputtering before the XPS measurement because the applied low ion energy cannot enable the
31 Ar ions to penetrate the target. The deposited films showed a thin TiO_2 coverage that was
32 composed due to the air exposure after deposition. The bulk composition of TiC films was
33 determined by XPS after removing the surface contamination and the oxide part by ion
34 sputtering (Tab. 1). The XPS measurement found weak oxygen signal in the films. The
35 quantities that can be calculated from the measured intensities are 2-4% which increases with
36 the Ti content of the layer. The measurement condition also made it possible to adsorb some
37 oxygen from the vacuum environment at the active sputtered surface of TiC. Thus, this
38 measurement is unable to identify the origins of the detected oxygen. The measured oxygen
39 means an upper limit of oxygen content for the films.
40
41
42
43
44
45

46 3.2. Mechanical properties

47

48 The load-depth curves obtained by indentation were evaluated for the hardness (H)
49 and the Young's modulus (E) by the method of Oliver and Pharr [20]. Characteristic load-
50 depth curves for different Ti powers are shown in Fig. 3. The hardness and the elastic
51 modulus of TiC nanocomposite thin films showed a distinct variation depending on metal
52 target power (see Table 2). It is revealed that both hardness and Young's modulus increase
53 with the increasing of the Ti target power. The increment is higher for lower power values.
54 The sample prepared at the power of 50 W has the highest nanohardness of ~ 66 GPa and
55 Young's modulus of ~ 401 GPa. The extremely high hardness of the current films might be due
56 to the composition variation and the small grain size of the reinforcing TiC nanocrystallites.
57 In comparison, the hardness and the Young's modulus of bulk TiC ceramic material are 30
58
59
60
61
62
63
64
65

1 GPa [21] and 439.43 GPa [22], respectively. It is noted that the nanohardness values can not
2 be compared directly with the hardness determined at larger forces the hardness increases
3 proportionately with decreasing test force (referred to as indentation size effect (ISE) [23]).
4 Similar high nanohardness values of ~66 GPa were obtained by Wang et al. [10] on TiC/a:C
5 films prepared by filtered cathodic vacuum arc technique. Gulbinski et al. [24] and Zehnder et
6 al [25] showed that with varying Ti concentration in TiC films prepared by reactive
7 magnetron sputtering of the sample containing about 50 at.% Ti possessed the maximal
8 microhardness of about 25 GPa.
9

10 Nedfors et al. [26] showed a decrease of the elastic modulus with the increase of
11 carbon content (increase of a-C phase) for Ti-C based coatings. The ratio between the
12 hardness and elastic modulus (H/E ratio) gives an indication of the nanocomposite coating's
13 wear resistance [27]. In the present experiments the H/E ratio of the TiC/a-C coatings showed
14 values between 0.153 and 0.164. These values are three times higher than the H/E (~0.05) is
15 for the films prepared by Nedfors et al. [26]. At the same time, the H/E obtained by Wang et
16 al. [10] on TiC/a:C films prepared by filtered cathodic vacuum arc technique has a similar
17 value of ~0.13 which is determined for the present materials.
18
19
20
21

22 3.3. Structural characterization

23
24 Cross-sectional TEM investigations were performed on TiC/a:C thin films. These
25 investigations confirmed that all thin films consist of nanometer-sized columnar TiC
26 crystallites embedded in carbon matrix. The average size of TiC crystallites and the thickness
27 of carbon matrix have been found to correlate with Ti content in the films, as will be shown
28 below. The difference between the structures of the films prepared at 20 W and 40 W Ti
29 power is illustrated in Fig. 4.
30

31 The TEM investigation of film prepared at 20 W Ti unthoughted an „amorphous”
32 character of films, because the content of TiC crystallites are extremely small (Fig. 4a). The
33 HREM investigation confirmed that this film consisted of 2-5 nm TiC crystallites embedded
34 in ~ 10 nm thick amorphous carbon (Fig. 4a). However, the formation of TiC columns was
35 started, but this growth was stopped for low content of Ti atoms compared with C atoms (Tab.
36 3) during deposition process. The film deposited at two times higher Ti power (40 W) showed
37 10-15 nm thick TiC columns and a few nanometer thick carbon matrix between the TiC
38 columns. The Selection Area Electron Diffraction (SAED) confirmed the presence of the
39 cubic TiC phase (Fig. 4b). The compositions of the TiC/a:C thin films determined by EDS
40 were shown in Tab.3. These values are in accordance with the data determined by XPS. In
41 case of EDS, the content of oxygen was lower than the detection limit. Similar results were
42 observed in our previous work [17, 28].
43
44
45

46 The film deposited at 20 W had a low Ti content of ~8 at.% while the film deposited at
47 40 W contained four times higher Ti content (30.4 at.%). EDS and XPS measurements are in
48 good correlation with the structure analysis. The increment in the Ti content was accompanied
49 by the increase of the amount of TiC nanoparticles which became rougher at higher Ti power.
50
51

52 4. Conclusions

53
54 TiC/a:C thin films were deposited by DC magnetron sputtering at 25 °C in argon
55 atmosphere. The films had a thickness of 400 nm and consisted of nanocrystalline TiC and
56 amorphous carbon phases. The average size of TiC crystallites and the thickness of the
57 amorphous carbon matrix strongly depended on deposition parameters, namely on Ti target
58 power. Films deposited at 15 W Ti power consisted of few nanometers small TiC
59
60
61
62
63
64
65

1 nanocrystallites embedded in a few ten nanometers thick carbon matrix. The increase of Ti
2 content (with increasing Ti power) resulted in larger TiC nanocrystallites and a thinner carbon
3 spacing between the TiC phases. This structural observation correlated with the concentration
4 determined by XPS and EDS measurements. The XPS signal of carbon was decomposed for
5 graphite and carbide according to their binding energies. This observation correlated with
6 Raman measurements. These results confirmed that all Ti atoms were bonded to C.

7 The nanohardness of TiC/a:C thin films increased proportionately with the TiC
8 crystallite content measured in the films. The highest nanohardness of 66 GPa and elastic
9 modulus of 401 GPa were observed in the film prepared at 50 W, which consisted of 15 nm
10 thick TiC columns separated by a 2-3 nm thin amorphous carbon matrix. The extremely high
11 hardness of the films may be due to the large amount and the small grain size of TiC
12 nanocrystallites.
13

14 **5. Acknowledgements**

15
16 This work was supported by the Hungarian Scientific Research Fund, OTKA, Grant No. K-
17 109021, the OTKA Postdoctoral grant Nr. PD 101453, the János Bolyai Research Scholarship
18 of the Hungarian Academy of Sciences. The research leading to this result has received
19 funding for European Community Seven Framework Programme FP7/2007-2013 under grant
20 agreement Nr. 602398 (HypOrth). Nikolett Oláh thanks to FIKU. The authors are grateful to
21 Mr. Péter Szommer for performing nanohardness measurements.
22
23
24
25
26

27 **References**

- 28
29
30 [1] Pei Y.T., Galvan D., De Hosson J. Th. M. Nanostructure and properties of TiC/a-C:H
31 composite coatings. *Acta Mater* 2005;**53**: 4505–4521.
32
33 [2] Jacobson B.E., Deshpandey C.V., Doerr H.J., Karim A.A., Bunshah R.F. Microstructure
34 and hardness of Ti (C, N) coatings on steel prepared by the activated reactive evaporation
35 technique. *Thin Solid Films* 1984;**118**: 285.
36
37 [3] Voevodin A.A., Prasad S.V., Zabinski J.S. Nanocrystalline carbide/amorphous carbon
38 composites. *J Appl Phys* 1997;**82**: 855-858.
39
40 [4] Patscheider J., Zehnder T., Diserens M. Structure-performance relations in nanocomposite
41 coatings. *Surf Coat Technol* 2001;**146-147**: 201-208.
42
43 [5] Gabriel H.M., Kloos K.H. Morphology and structure of ion-plated TiN, TiC and Ti (C, N)
44 coatings. *Thin Solid Films* 1984;**118**: 243.
45
46 [6] Matthews A., Eskildsen S.S. Engineering applications for diamond-like carbon, *Diamond*
47 *Relat Mater* 1994;**3**: 902.
48
49 [7] Roth D., Rau B., Roth S., Mai J., Dittrich K.H. Large area and three-dimensional
50 deposition of diamond-like carbon films for industrial applications. *Surf Coat Technol*
51 1995;**74-75**: 637.
52
53 [8] Shtansky DV, Gloushankova NA, Bashkova IA, Petrzhik MI, Sheveiko AN,
54 Kiryukhantsev-Korneev PhV, et al. Multifunctional biocompatible nanostructured coatings
55 for load-bearing implants. *Surf Coat Technol* 2006;**201**: 4111-8.
56
57 [9] Balázs K., Vandrovcová M., Bačáková L., Balázs C., Bertóti I., Davin F. and Radnóczy
58 G. Mechanical behavior of bioactive TiC nanocomposite thin films. *Mater Sci Forum*
59 2013;**729**: 296-301.
60
61
62
63
64
65

- 1 [10] Wang Y., Zhang X., Wu X., Zhang H., Zhang X. Compositional, structural and
2 mechanical characteristics of nc-TiC/a-C:H nanocomposite films. *Appl Surf Sci* 2008;**255**:
3 1801-1805.
- 4 [11] El Mel A.A., Angleraud B., Gautron E., Garnier A., Tessier P.Y. XPS study of the
5 surface composition modification of nc-TiC/C nanocomposite films under in situ argon ion
6 bombardment. *Thin Solid Films* 2011;**519**: 3982-3985.
- 7 [12] Wang H.L., He J.L., Hon M.H. Sliding wear resistance of TiCN coatings on tool steel
8 made by plasma-enhanced chemical vapour deposition. *Wear* 1993;**169**: 195.
- 9 [13] Lackner JM, Waldhauser W, Ebner R. Large-area high-rate pulsed laser deposition of
10 smooth TiC_xN_{1-x} coatings at room temperature-mechanical and tribological properties. *Surf*
11 *Coat Technol* 2004;**188**: 519-24.
- 12 [14] Galvan D, Pei YT, De Hosson JTM. Influence of deposition parameters on the structure
13 and mechanical properties of nanocomposite coatings. *Surf Coat Technol* 2006;**201**: 590-8.
- 14 [15] Sedláčková K., Ujvári T., Grasin R., Lobotka P., Bertóti I., Radnóczy G. C-Ti
15 nanocomposite thin films: Structure, mechanical and electrical properties. *Vacuum* 2008;**82**:
16 214-216.
- 17 [16] Musil J. Hard and superhard nanocomposite coatings. *Surf Coat Technol* 2000;**125**: 322.
- 18 [17] Balázs K., Vandrovcová M., Bačáková L., Balázs Cs. Structural and biocompatible
19 characterization of TiC/a:C nanocomposite thin films. *Mat Sci Eng C* 2013; **33**: 1671-1675.
- 20 [18] Amer M., Barsoum M. W., El-Raghy T., Weiss I., Leclair S. et al. *J Appl Phys* 1998;**84**:
21 5817.
- 22 [19] Christ B.W., Handbook of Monochromatic XPS spectra, Wiley, New York, 2000.
- 23 [20] Oliver W.C., and Pharr G.M. An improved technique for determining hardness and
24 elastic modulus using load and displacement sensing indentation experiments. *J Mater Res*
25 1992;**7**: 564-1583.
- 26 [21] Krajewski A., D'Alessio L. and De Maria G. Physico-Chemical and Thermophysical
27 Properties of Cubic Binary Carbides. *Cryst Res Technol* 1998;**33**: 341.
- 28 [22] <http://www.memsnet.org/material/titaniumcarbidebulk/>
- 29 [23] Nino A., Tanaka A., Sugiyama S. and Taimatsu H. Indentation Size Effect for the
30 Hardness of Refractory Carbides. *Mat Trans* 2010;**51**: 1621.
- 31 [24] Gulbiński W., Mathur S., Shen H., Suszko T., Gilewicz A., Warcholiński B. Evaluation
32 of phase, composition, microstructure and properties in TiC/a-C:H thin films deposited by
33 magnetron sputtering. *Appl Surf Sci* 2005; **239(3-4)**: 302-306.
- 34 [25] Zehnder T., Schwaller P., Munnik F., Mikhailov S., and Patscheider J. Structure-
35 performance relations in nanocomposite coatings. *J Appl Phys* 2004;**95**: 4327.
- 36 [26] Nedfors N., Tengstrand O., Lewin E., Furlan A., Eklund P., Hultman L. and Jansson U.
37 Structural, mechanical and electrical-contact properties of nanocrystalline-NbC/amorphous- C
38 coatings deposited by magnetron sputtering. *Surf Coat Tech* 2011;**206**: 354-359.
- 39 [27] Leyland A., Matthews A. Review: plasma electrolysis for surface engineering. *Wear*
40 2000;**246**: 1-11.
- 41 [28] Balázs K., Lukács I.E., Gurbán S., Menyhárd M., Bačáková L., Vandrovcová M.,
42 Balázs C. Structural, mechanical and biological comparison of TiC and TiCN
43 nanocomposites films. *J Eur Ceram Soc* 2013;**33**: 2217-2221.
- 44
45
46
47
48
49
50
51
52
53
54
55
56
57
58
59
60
61
62
63
64
65

Ti power	15 W	20 W	30 W	40 W	50 W
Ti (at.%)	16.3 ± 4	22.1 ± 3	28.6 ± 3	33.4 ± 3	39.7 ± 4
C carbide (at.%)	8.2 ± 5	16.5 ± 3	21.9 ± 4	38.6 ± 4	44.3 ± 5
C graphite (at.%)	69.2 ± 5	54.2 ± 2	42.8 ± 3	21 ± 2	8.1 ± 5
O (at.%)	2.8 ± 1	2.5 ± 1	3.3 ± 1	3.9 ± 1	4.1 ± 1
Ar (at.%)	3.4 ± 1	4.7 ± 1	3.4 ± 1	3.1 ± 1	3.7 ± 1

Tab. 1.

Ti power	15 W	20 W	30 W	40 W	50 W
H (GPa)	36 ± 6	50 ± 7	59 ± 16	59 ± 9	66 ± 18
E (GPa)	235 ± 19	287 ± 19	325 ± 25	344 ± 30	401 ± 52
H/E	0.153	0.174	0.182	0.171	0.164

Tab. 2.

Ti power	15 W	20 W	30 W	40 W	50 W
Ti (at.%)	8.1	15.8	23.7	30.4	48.6
C (at.%)	91.9	84.2	76.3	69.6	50.9

Tab. 3.

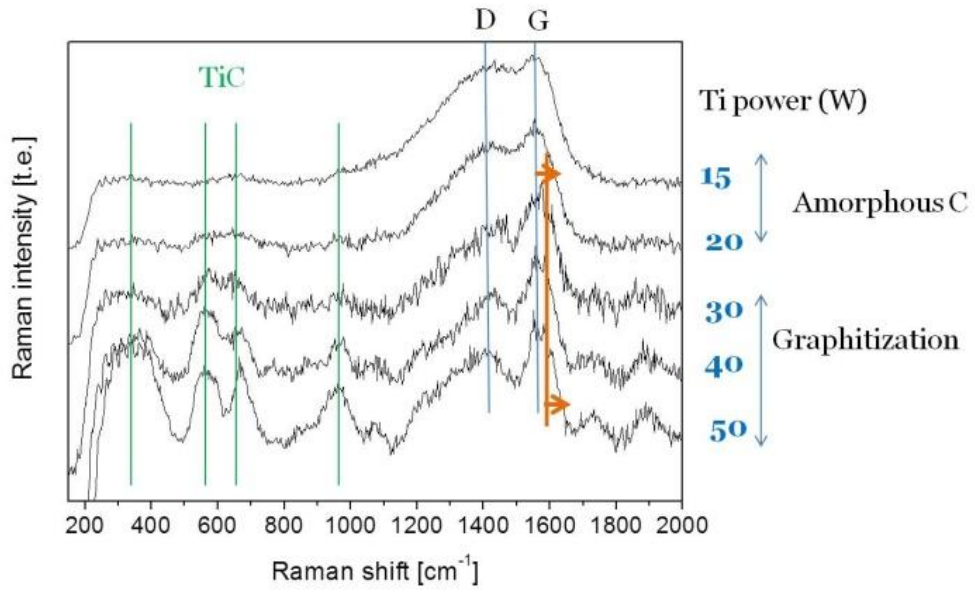


Fig. 1.

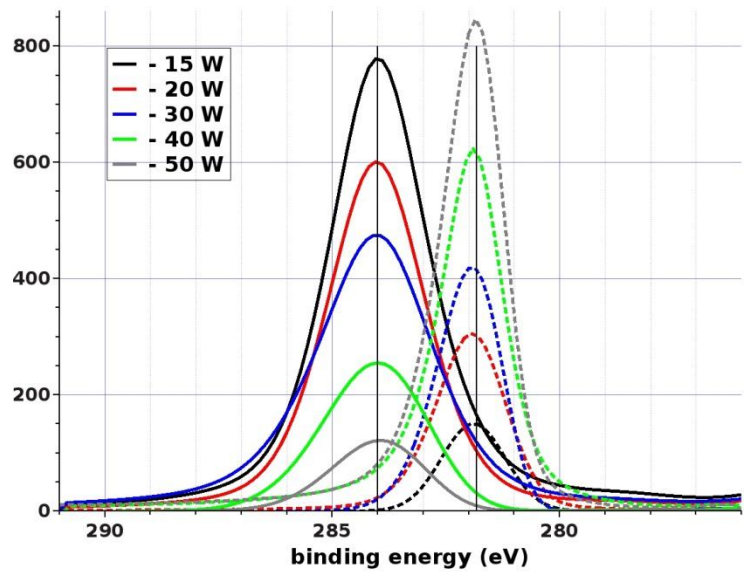


Fig. 2.

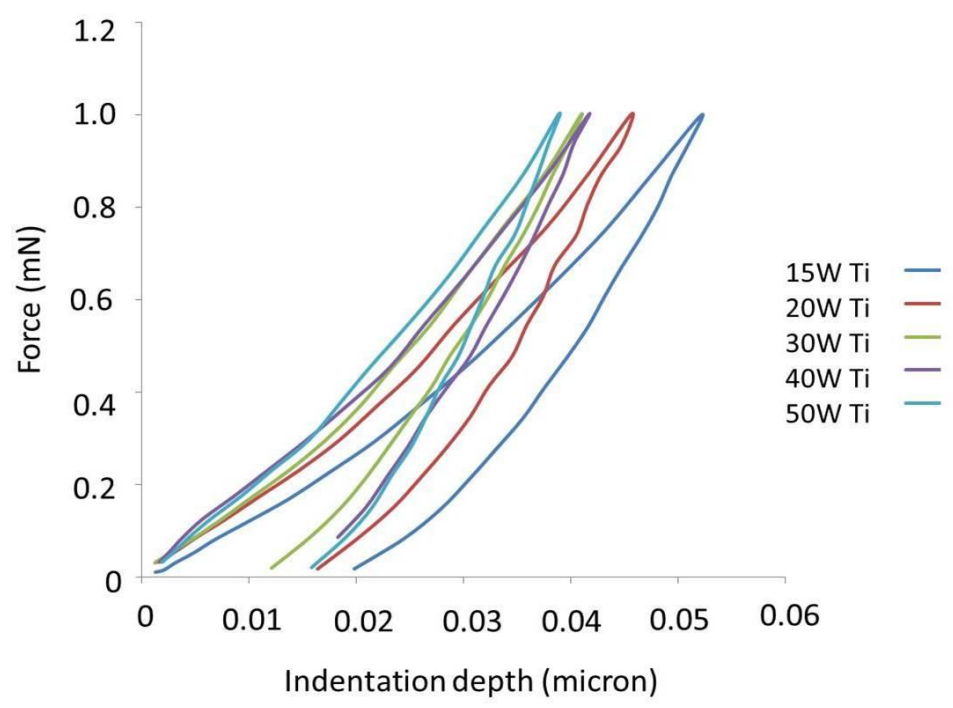


Fig. 3.

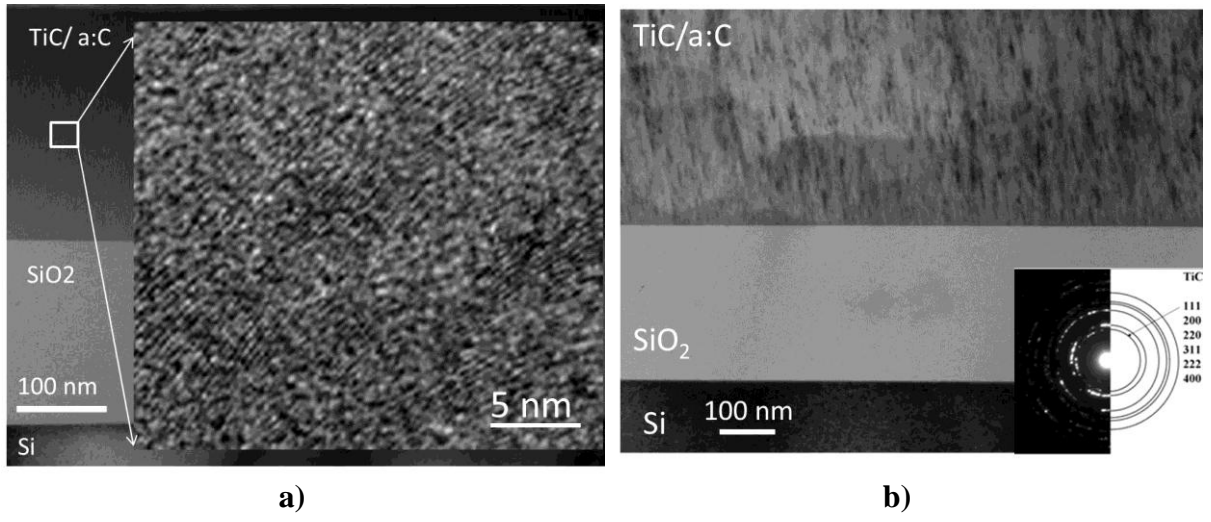


Fig.4.

Figure Captions

1
2 **Fig. 1.** The Raman spectroscopy measurement of TiC based nanocomposite thin films
3 prepared by Ti power between 15 and 50 W.
4

5
6 **Fig. 2.** Decomposed C 1s line from XPS spectra of the different TiC/a:C films. Bold line:
7 graphite components, dashed line: carbide components. The curves with the same color
8 belong to the same specimen, and the graphite and carbide components are drawn with solid
9 and dashed lines, respectively.
10

11
12 **Fig. 3.** Characteristic load-depth curves obtained by nanoindentation for TiC based
13 nanocomposite thin films prepared at various Ti powers (15-50 W).
14

15
16 **Fig. 4.** Cross-sectional TEM image of TiC/a:C thin films prepared at various Ti powers.
17 a) 20 W (The detail shows the HREM image with nanosized TiC crystallites embedded in
18 amorphous carbon matrix), b) 40 W (SAED in details confirmed the cubic TiC phase).
19

Table

20
21
22 **Tab. 1.** Concentration of components in the TiC based nanocomposites prepared at various Ti
23 power as determined from XPS peaks.
24

25
26 **Tab. 2.** The hardness (H), the Young's modulus (E) and the ratio between the two quantities
27 (H/E).
28

29
30 **Tab. 3.** The elemental composition of the TiC based nanocomposite films. The error is $\pm 2\%$.
31
32
33
34
35
36
37
38
39
40
41
42
43
44
45
46
47
48
49
50
51
52
53
54
55
56
57
58
59
60
61
62
63
64
65